ELSEVIER

Thermochimica Acta 388 (2002) 327–341

thermochimica acta

www.elsevier.com/locate/tca

Modeling and experimental verification of the kinetics of reacting polymer systems

G. Van Assche, S. Swier, B. Van Mele*

Department of Physical Chemistry and Polymer Science, Vrije Universiteit Brussel, Pleinlaan 2, 1050 Brussels, Belgium

Received 1 July 2001; received in revised form 16 November 2001; accepted 19 November 2001

Abstract

Diffusion limitations have an impact on epoxy cure reactions near vitrification. The effects of diffusion control on the rate of reaction can be described by the evolution of a mobility factor, which is directly based on the experimental heat capacity evolution measured with differential (scanning) temperature modulated calorimetry (D(S)TMC) as diffusion and mobility factor coincide for the epoxy resins studied. A model based on the free volume theory and the Rabinowitch activated complex theory is presented here. It relates the apparent rate constant to the difference between the reaction temperature and T_g. Very good correlations are derived between model calculations and the experimental normalized mobility factor measured at 1/60 Hz. A further extension of the model to allow for experimental mobility factors measured at different modulation frequencies is also proposed. The model successfully predicts the deceleration of reactions due to diffusion limitations, which demonstrates the applicability of D(S)TMC to estimate the effect of the reaction-induced vitrification on the polymerization and to model the overall cure kinetics.

Keywords: Differential scanning temperature modulated colorimetry; Reaction kinetics; Modeling; Vitrification; Diffusion control

1. Introduction

The network formation of thermosetting polymer systems often depends on both chemical reactivity and mobility of the reactive units. This mobility is influenced by the visco-elastic state of the changing material. *Vitrification* of the developing polymer network occurs when the glass transition, T_g of the reacting system reaches the cure temperature due to the increase in molecular weight or crosslink density. This transformation involves the change of the material from a *mobile* liquid or rubbery state to a *frozen* glassy state. Due to the attendant decrease of the chain segment mobility the reaction becomes *diffusion-controlled*. This eventually leads to a complete halt of the reaction, with residual reactive units as a consequence. As chemical, mechanical and electrical properties attain their ultimate value during the last stages of the cure process, the diffusion-controlled regime appears to be a very important part. An accurate quantitative description of the impact of mobility restriction on cure is therefore essential.

1.1. Cure kinetics by DSC and D(S)TMC

Differential scanning calorimetry (DSC) is a very elegant and widely applied technique for measuring an overall extent of conversion for chemical reactions. It is not as time consuming as alternative direct analysis methods [1–3].

* Corresponding author. Tel.: +32-2-6293276; fax: +32-2-6293278.
E-mail address: bvmele@vub.ac.be (B. Van Mele).

0040-6031/02/$ – see front matter
PII: S0040-6031(02)00038-2

If the exothermic heat evolved during chemical reaction is proportional to the extent of consumption of reactive groups, the *overall conversion*, x, and the *overall rate of conversion*, dx/dt, can be calculated as:

$$x = \frac{\Delta H_t}{\Delta H_{tot}} \quad (1)$$

and

$$\frac{dx}{dt} = \frac{1}{\Delta H_{tot}} \frac{dH}{dt} \quad (2)$$

with ΔH_t the overall reaction enthalpy evolved up to time t and ΔH_{tot} the overall reaction enthalpy for full reaction ($x = 1$) or total reaction enthalpy. The reaction kinetics can be studied in both isothermal and non-isothermal conditions.

An alternative evaluation of the cure process by DSC can be achieved by performing partial and residual cure experiments. In a partial cure experiment, at a predetermined time or temperature (for isothermal or non-isothermal cure conditions) the sample is quenched to a much lower temperature in order to stop the chemical reactions. In a subsequent heating experiment, termed the *residual cure* experiment, the glass transition, T_g and the residual reaction enthalpy, ΔH_{res} are measured. The overall conversion x at the predetermined time or temperature is then calculated as:

$$x = \frac{\Delta H_{tot} - \Delta H_{res}}{\Delta H_{tot}} \quad (3)$$

Because of the existence of a one to one relationship between T_g and x [4], it can be more adequate to use T_g instead of ΔH_{res}, especially towards complete conversion as ΔH_{res} is small and difficult to quantify in these conditions. It should be noted, however, that any method that involves increasing the temperature of a partially cured sample may allow cure reactions to proceed, thus T_g may increase while it is being measured.

In previous work, differential (scanning) temperature modulated calorimetry (D(S)TMC) proved to be very advantageous for studying the cure and vitrification of thermosetting systems [5–9]. In this extension of DSC, the heat capacity is measured simultaneously with the heat flow by superimposing a small temperature modulation onto the isothermal or non-isothermal temperature program. Hence, simultaneously with the reaction exotherm observed in the heat flow, the reaction-induced vitrification can be studied from a step-wise decrease in heat capacity. This decrease and the corresponding relaxation peak in the heat flow phase are attributed to the reaction-induced loss of segmental conformational contributions in the glass transition region. This occurs when the characteristic time-scale of the molecular relaxations, associated with the co-operative movements in the glass transition region, becomes longer than the modulation period (or the characteristic time-scale of the experiment) [10].

For the polymerization of epoxy systems the diffusion control is non-specific (or overall) [11]. This means that the diffusion control is determined by a single (or average) mobility, the chain segment mobility.

1.2. Model for cure kinetics including diffusion control

Because diffusion limitations and/or mobility restrictions often complicate the cure kinetics, the effect of diffusion has to be incorporated into the overall reaction rate law. One approach to quantify the effects of diffusion or mobility restrictions on the cure kinetics is via direct estimation of a diffusion factor, DF. The latter is defined as the ratio of the experimentally measured conversion rate, $(dx/dt)_{obs}$ over the predicted conversion rate at the *same* reaction conversion x in the absence of mobility restrictions $(dx/dt)_{kin}$:

$$\left(\frac{dx}{dt}(x,T)\right)_{obs} = DF(x,T)\left(\frac{dx}{dt}(x,T)\right)_{kin} \quad (4)$$

where $(dx/dt)_{obs}$ is proportional to the heat flow measured in DSC (see Eq. (2)) and T is the absolute temperature. For the chemically controlled reaction rate of an epoxy resin cure showing autocatalytic behavior, the empirical rate equation proposed by Kamal [12] can be applied:

$$\left(\frac{dx}{dt}\right)_{kin} = (k_1 + k_2 x^m)(1-x)^n = k_{kin}(1-x)^n \quad (5)$$

with x the conversion of epoxy groups, k_1 and k_2 the rate constants, m and n the reaction orders. The temperature dependence of the rate constants k_1 and k_2

is given by an Arrhenius relationship:

$$k = A \exp\left(-\frac{E}{RT}\right) \tag{6}$$

with A the pre-exponential factor, E the activation energy, and R the universal gas constant. The phenomenological 'rate constant' $k_{kin}(x, T)$ is describing the overall, chemically controlled polymerization reaction and is incorporating an increase in value due to autocatalysis.

Combining Eqs. (4) and (5) results in:

$$\left(\frac{dx}{dt}\right)_{obs} = DF(x,T) k_{kin} (1-x)^n = k_{app} (1-x)^n \tag{7}$$

$$k_{app} = k_{kin}\, DF(x,t) \tag{8}$$

with $k_{app}(x, T)$ an *apparent* rate constant including the effect of diffusion on $k_{kin}(x, T)$. Note again that k_{app} is not a true rate constant.

A quantification of DF to describe the transition from chemically controlled to diffusion-controlled kinetics is based on the Rabinowitch equation which is derived from the activated complex theory [12–15]. Two reactive groups diffuse toward each other to form an activated complex with possible creation of a stable bond. Whether the reaction is controlled by diffusion depends on the relative time to diffuse and the time needed for the intrinsic chemical reaction resulting in bond formation:

$$t_{reaction} = t_{diffusion} + t_{chem\ \ kin} \tag{9}$$

or

$$\frac{1}{k_{app}} = \frac{1}{k_D} + \frac{1}{k_{kin}} \tag{10}$$

with k_D a rate constant for diffusion. As long as diffusion in and out of the complex occurs more frequently than the process of bond formation, the reaction is controlled by chemical kinetics, $k_{app} = k_{kin}$ or $t_{reaction} = t_{chem\ \ kin}$ for $k_D \gg k_{kin}$. In the other limiting case, $k_{app} = k_D$ or $t_{reaction} = t_{diffusion}$ for $k_D \ll k_{kin}$. The frequency of collisions leading to reaction in conditions excluding and including diffusion limitations is thus expressed by k_{kin} and k_{app}, respectively.

Combining Eqs. (8) and (10) results in the following equation for the diffusion factor:

$$DF(x,T) = \frac{k_D(x,T)}{k_D(x,T) + k_{kin}(x,T)} \tag{11}$$

The diffusion rate constant, k_D can be expressed in terms of the overall diffusion coefficient, D [16]:

$$k_D = k_{D0}(T)\, D(x,T) \tag{12}$$

with $k_{D0}(T)$ a constant related to local conditions for creation of the chemical bond. For the step-growth polymerization reactions of an amine-cured epoxy the overall diffusion of reactive groups toward each other is governed by the diffusion of chain segments. Thus, the overall diffusion coefficient, D is expected to be inversely proportional to the relaxation time of polymer segments [17], which enables a model based on the free volume concept and a description similar to the Williams–Landel–Ferry (WLF) equation [18–21]:

$$D = D_0 \exp\left(\frac{C_1 (T - T_g)}{C_2 + T - T_g}\right) \tag{13}$$

with C_1 and C_2 constants depending on the epoxy system.

Employing an Arrhenius temperature dependency for $k_{D0}(T)$ the equation for the diffusion rate constant, k_D is finally given by:

$$\ln k_D(x,T) = \ln A_D - \frac{E_D}{RT} + \frac{C_1 (T - T_g(x))}{C_2 + T - T_g(x)} \tag{14}$$

with A_D the pre-exponential factor and E_D the activation energy for the diffusion rate constant k_{D0}. Note that k_D equals k_{D0} for T_g equal to T. For k_{D0}, a similar Arrhenius dependency is proposed in literature, but instead of the WLF free volume contribution a more empirical approach was used [22]. The Arrhenius temperature dependency for $k_{D0}(T)$ will also be justified by the results.

Note that all the activation energies in the model are constant and thus conversion independent. Nevertheless, the global activation energy of the overall reaction process, associated with k_{app} (Eq. (7)) and also k_{kin} (Eq. (5)), is an *apparent* and conversion-dependent value (a concept discussed in, e.g. [23]).

In the case of a curing system, the value of T_g is a function of the reaction conversion. The following equation was used [24,25]:

$$T_g(x) = \frac{T_{gu}}{1 - K_C X_C} = \frac{T_{go} + a\,x}{1 - K_C X_C} \tag{15}$$

with a and K_C the optimization parameters, T_{go} the glass transition temperature of the unreacted mixture

and X_C the crosslink density. X_C equals 0 as long as x is below x_{gel} and rises up to 1 from x_{gel} to the final conversion of 1. K_C in the denominator is describing the effect of crosslinking on T_g. T_{gu} is the glass transition temperature of an uncrosslinked system identical in every respect to the crosslinked system except that the crosslinks are missing. The parameter a in T_{gu} describes the effect of the decrease of the concentration of chain ends on T_g.

1.3. Model optimization strategy

The fitting strategy to optimize the model parameters involves the *simultaneous* treatment of *all* isothermal and non-isothermal cure experiments with and/or without mobility restrictions of a thermosetting system of a *fixed* initial composition (e.g. stoichiometric mixtures). The temperature range is largely extended to obtain an accurate estimate for all fitting parameters of the cure rate model.

The modeling was performed using FITME, a version of OPTKIN [26], a program for the mechanistic modeling of reaction kinetics, modified to enable the calculation (*simulation*) and fitting (*optimization*) of conversion and rate of conversion profiles, and other profiles related to these, for isothermal, non-isothermal, and user-defined temperature programs. The optimum set of parameters derived corresponds to the least sum of squares of the differences between experimental and calculated values. This non-linear multiple parameter regression uses an algorithm based on a combination of the methods of Newton–Raphson, Steepest Descent and Marquardt [27,28]. It requires no assumptions (apart from the proposed cure rate law with kinetic and diffusion effects) and can therefore be applied to many kinds of cure reactions.

The model parameters are summarized below:

Chemical kinetics (see Eq. (5))	A_1, $E_1(k_1)$, A_2, $E_2(k_2)$, m, n
Diffusion model (see Eqs. (11) and (14))	A_D, $E_D(k_{D0})$, C_1, C_2
T_g–x relation (see Eq. (15))	T_{go}, a, K_C, $x_{gel}(X_C)$

During the regression analysis, the model parameters can be kept within physically acceptable limits.

2. Experimental

2.1. Materials

A bifunctional epoxy (diglycidyl ether of bisphenol A, LY 556, Ciba–Geigy) and a tetrafunctional epoxy (N,N,N',N'-tetraglycidyl-4,4′-diaminodiphenylmethane, MY 720, Ciba–Geigy) have been studied. The curing agents combined with these epoxy resins are, respectively an anhydride hardener (methyltetrahydrophthalic anhydride HY 917, Ciba–Geigy) using 1 wt.% of an accelerator (1-methyl imidazole, DY 070, Ciba–Geigy), and a tetrafunctional amine hardener (3,3′-dimethyl-4,4′-diaminodicyclohexylmethane, HY 2954, Ciba–Geigy). In this paper only stoichiometric mixtures will be discussed.

2.2. Instruments

A TA Instruments 2920 DSC with MDSC™ option and RCS was operated in MDSC™ mode at a frequency of 1/60 Hz with amplitudes ranging between 0.1 and 1 °C. The instrument was calibrated for temperature, enthalpy, and heat capacity using appropriate reference materials.

2.3. Considerations for accurate kinetic analysis

2.3.1. Sample preparation, sample size and storage

Reactive mixtures were prepared in the correct weight ratios. Precautions have to be taken in order to avoid reaction prior to the D(S)TMC experiment. One procedure might be to mix all components at room temperature and to store this mixture at low temperature (e.g. −20 °C) before analysis. The recommended procedure, however, is to use freshly prepared reaction mixtures for which the initial conversion approaches zero. A sample mass of 5–10 mg was selected as a compromise between the thermal detection limit and the existence of thermal gradients in the sample.

2.3.2. Temperature window for (quasi-)isothermal experiments

For a quantitative analysis of the reaction kinetics, the selection of appropriate isothermal cure temperatures is important. At too low cure temperatures, the reaction rate is too slow and the corresponding heat flow data may not exceed baseline noise. At too high cure temperatures, the reaction rate is too fast, so that a significant degree of conversion is unrecorded in the equilibration period at the start of the experiment.

The sample can be immediately inserted into the DSC furnace which is previously equilibrated at the desired curing temperature, or the sample can be placed into the DSC furnace at room temperature and then heated to the required temperature at a rapid but controlled rate. With both methods, however, some heat of reaction might remain unrecorded in the initial equilibration period and an extrapolation to zero time is needed for accurate kinetic data.

2.3.3. Non-isothermal versus isothermal experiments

Fundamental kinetic studies are by preference performed in isothermal rather than in non-isothermal reaction conditions because frequently, as cure proceeds, parallel reactions with different activation energies occur, changing the relative rates of reactions with temperature. In theory, one non-isothermal experiment comprises all the kinetic information normally enclosed in a series of isothermal experiments, which makes the kinetic analysis of non-isothermal DSC data very attractive. The criteria for judging the kinetic parameters derived from non-isothermal experiments must be the ability to describe the isothermal experiments as well. Yet, in practice, the parameters derived from the kinetic analysis of one non-isothermal experiment are inaccurate; the activation energy and the pre-exponential factor are generally overestimated. If several non-isothermal experiments are considered, more accurate values for the activation energy and the pre-exponential factor are obtained [29,30]. A lot of discrepancies among the parameters derived from isothermal and non-isothermal experiments are ascribed to the thermal lag of the instrument when a heating rate is applied [31]. However, a lot of the unreliability comes from attempting to fit measured data to a kinetic equation that does not truly describe the real course of the reaction.

To maximize the experimental temperature window, a combination of isothermal and non-isothermal experiments is preferred in this work.

2.3.4. Baseline selection

The calculation of conversion (Eq. (1)) and conversion rate (Eq. (2)) requires the numerical integration of the (partial) areas of exothermic reaction peaks and therefore the need to draw a baseline.

For isothermal DSC data, the heat flow signal goes asymptotically to a plateau value when the reaction is completed. Because it is difficult to separate residual reaction from instrumental instability at this final stage, it is useful to let any reaction that appears to be completed at time t, continue for a time $2t$. The baseline is a horizontal at this final steady state signal.

For non-isothermal DSC data, the baseline can be approximated as linear. However, if there is a significant change in heat capacity between reactants and products, $\Delta C_{p,\,\mathrm{react}}$, a better approach might be to assume a baseline proportional to the reaction conversion [2]. In this context, D(S)TMC has the advantage that both heat capacity and heat flow are measured. A non-reversing heat flow signal is calculated which contains the change in heat flow due to chemical reaction only. A second heating experiment for the fully cured resin provides additional indications for the beginning and the end of the baseline.

2.3.5. Total reaction enthalpy

The overall reaction enthalpy at full conversion or total reaction enthalpy, ΔH_{tot} is an important quantity for the calculation of conversion and conversion rate in Eqs. (1) and (2). During an isothermal cure well below $T_{\mathrm{g}\infty}$ or $T_{\mathrm{g},x=1}$, reactivity is frozen out and full conversion is never reached. Therefore, an accurate value of ΔH_{tot} is calculated from non-isothermal experiments and this preferably at multiple heating rate (e.g. between 5 and 20 $^{\circ}\mathrm{C\,min^{-1}}$). At a too low heating rate, some initial and final reaction may remain unrecorded because of insufficient instrument sensitivity. At a too high heating rate, the final stages of cure will interfere with thermal decomposition processes.

It is important to note that at an advanced conversion the functional groups can no longer meet and react because of the progressively increasing topological complexity of a reacting system. Therefore, the

complete conversion of functional groups, i.e. full overall chemical conversion, may never be attained. Even in the complete absence of any diffusion hindrance, this topological constraint cannot be removed by a simple temperature rise. This is in contrast to reactions controlled by mobility restrictions related to the increasing relaxation time of the material, i.e. an isothermal cure at temperatures well below $T_{g,x=1}$. These mobility restrictions are removed by heating the sample above $T_{g,x=1}$. In the case of a topological limit, the experimental value of ΔH_{tot} is always lower than the theoretical limit, as calculated from the reaction heat of model compounds.

2.4. Considerations for D(S)TMC parameters

In a D(S)TMC experiment, a repeated temperature modulation is superimposed on the normal linear temperature program [32–37]. The modulation amplitude and frequency, and the underlying heating rate can be chosen independently.

To measure C_p accurately, it is advisable to use a modulation amplitude of 0.1–1 °C. The amplitude of the temperature modulation has to be limited, since its effect on the cure kinetics has to be negligible. For non-isothermal cure experiments 'heating only' conditions, with the modulation amplitude chosen sufficiently small to avoid cooling over one complete cycle, are of no use.

The range of frequencies that can be used in practice is limited to about one decade, so that no strong frequency effects are expected, as opposed to the conditions of dielectric measurements where frequencies can easily be changed from 1 to 10^5 Hz. The modulation frequency in all D(S)TMC experiments shown is always fixed at 0.017 or 0.01 Hz (corresponding to a modulation period of 60 or 100 s, respectively). The frequency dependence of the heat capacity during cure will be discussed in the last section.

3. Results and discussion

3.1. Cure and vitrification by D(S)TMC

In previous papers [5–7] the use of D(S)TMC for studying the cure and vitrification of thermosetting systems was discussed. Fig. 1 summarizes a typical experiment in quasi-isothermal conditions. The maximum in the reaction exotherm (heat flow) indicates the autocatalytic behavior of the system. A step-wise decrease in C_p starts near 160 min (for a 1/60 Hz modulation frequency; Fig. 1). The evolution of the glass transition T_g, determined by partial cure experiments, confirms that the decrease in C_p can be attributed to a reaction-induced vitrification that occurs when T_g increases up to T_{iso} (Fig. 2). The conversion x, obtained by partial numerical integration of the experimental heat

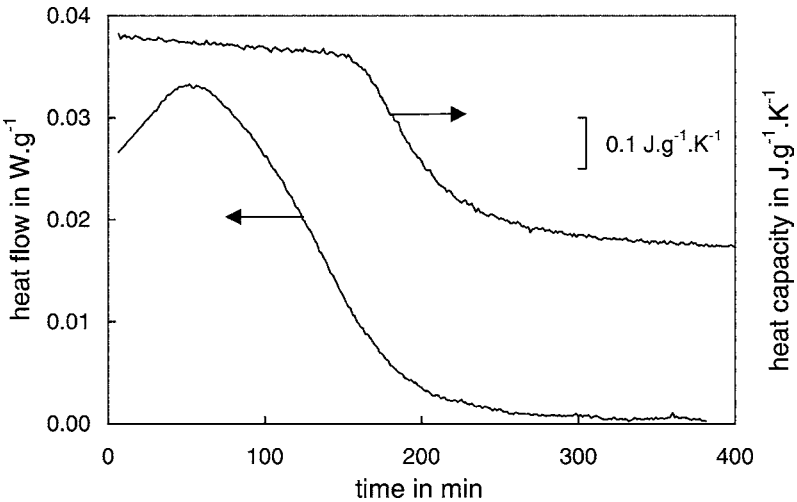

Fig. 1. Heat flow and heat capacity of quasi-isothermal cure of an epoxy–anhydride system at 85 °C.

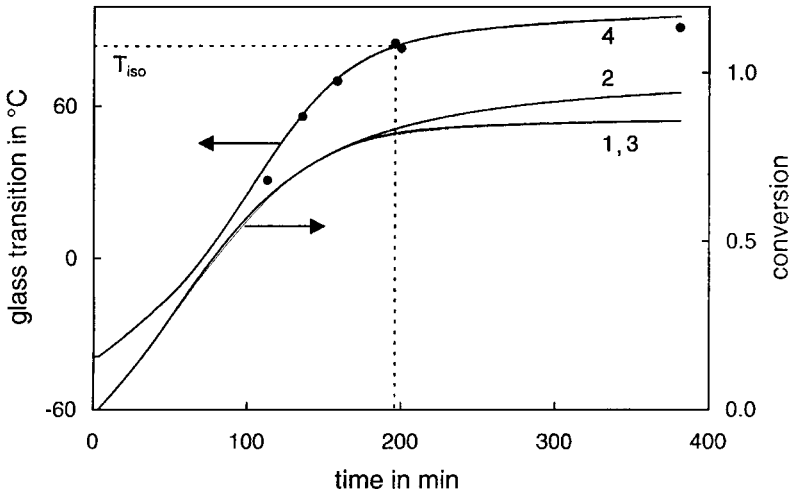

Fig. 2. Quasi-isothermal cure of an epoxy–anhydride system at 85 °C. Glass transition T_g: measured after partial cure (●) and (4) evolution using T_g–x relation (see Eq. (15)). Conversion x: (1) calculated from measured conversion rate $(dx/dt)_{obs}$ (see Eq. (2)); (2) calculated from $(dx/dt)_{kin}$ without diffusion control; (3) calculated from $(dx/dt)_{kin}$. $DF^*(t)$ with diffusion control; $(dx/dt)_{kin}$ is determined by kinetic modeling (see text); DF^* is the normalized heat capacity (see Eq. (16)).

flow signal (Eq. (1)), is reaching a limiting value less than 1 (Fig. 2, curve 1). Near vitrification the advance of conversion slows down and halts before full cure is reached. This is due to the onset of diffusion control of the cure reaction at T_{iso}. Note that the experimental values of T_g show an evolution as described by the relationship between T_g and x (Eq. (15)).

3.2. Model assumptions and experimental verification

3.2.1. Mobility factor as model for diffusion factor

The chemically controlled polymerization kinetics $(dx/dt)_{kin}$ was modeled by fitting the autocatalytic rate equation (Eq. (5)) to isothermal and non-isothermal rate of conversion profiles $(dx/dt)_{obs}$ (Eq. (2)), in regions of chemically controlled conditions (before the onset of vitrification, where $DF(x, T) = 1$). The diffusion factor $DF(x, T)$ was subsequently calculated as the ratio of the observed $(dx/dt)_{obs}$ over the modeled $(dx/dt)_{kin}$, according to Eq. (4).

To quantify the loss of (co-operative) mobility due to vitrification, a mobility factor DF^* was defined by normalizing the heat capacity:

$$DF^*(x, T) = \frac{C_p(x, T) - C_{pg}(x, T)}{C_{pl}(x, T) - C_{pg}(x, T)} \quad (16)$$

with C_{pl} and C_{pg} the heat capacities of the mobile and glassy reference states at the same conversion and temperature.

For both the anhydride-cured and the amine-cured systems discussed, the results show that DF (nearly) coincides with the normalized decrease in C_p (DF^*, measured at 1/60 Hz) for a wide range of cure temperatures and heating rates [5–7]. Consequently, the evolution of the mobility factor DF^* was proposed as a simultaneous, but independent, in situ measurement of the diffusion factor DF to describe quantitatively the decrease in the rate of reaction due to vitrification.

The validity of this proposal can be elaborated upon using Fig. 2, comparing the evolutions of conversion for experimental (1) and calculated curves (2 and 3). The evolution without diffusion control (curve 2) was calculated from Eq. (5) which was based on data before the onset of vitrification. The third curve was obtained from Eq. (4) using the chemical kinetics model (Eq. (5)) and with $DF^*(t)$ as a model for $DF(t)$. Over the whole conversion range, the conversion calculated using DF^* as a model for DF is practically identical to the measured curve, which supports the approach proposed.

Recent results from other groups [38,39] support these findings. This indicates that upon vitrification of these thermosetting resins, the characteristic times for

the molecular relaxations associated with the co-operative movement involved in the glass transition region (ca. 10^2 s), are comparable to those of the (reaction) rate-determining mobility upon transition to diffusion-controlled reaction conditions. The following observations support this point:

(a) For diffusion-controlled step-growth polymerization reactions of an amine-cured epoxy the overall diffusion of reactive groups toward each other is governed by the diffusion of chain segments (and not center-of-mass diffusion) [11].
(b) The distance between residual reactive epoxide functionalities is about 10 Å and the corresponding volume surrounding each residual reactive epoxide functionality contains about 50 carbon atoms (upon vitrification). This scale of magnitude is comparable to the co-operative movement of roughly 30–50 chain atoms involved in the glass transition.

The influence of the modulation frequency on the mobility factor and the consequences for the model will be discussed further on.

3.2.2. Temperature dependency of k_{D0}

Consider the isothermal cure of the epoxy–anhydride system at 85 °C (Fig. 1). If the mobility factor DF* is used as a first approximation of the diffusion factor DF, Eq. (11) results in the following equation for the diffusion rate constant k_D:

$$k_D = k_{\text{kin}}\left(\frac{\text{DF}^*}{1-\text{DF}^*}\right) \tag{17}$$

where the value of k_{kin} is obtained by chemical kinetic modeling (Eq. (5)) under conditions with no mobility restrictions ($\text{DF}(x,T)=1$), as discussed in the previous paragraph. Fig. 3 plots the thus obtained logarithm of the diffusion rate constant, $\log_{10} k_D$, as a function of $(T-T_g)/(C_2+T-T_g)$, with C_2 equal to 51.6 °C (universal value according to WLF approach). The intercept gives $\log_{10} k_{D0}$, while the slope gives C_1 (Eq. (14)). For Fig. 3, only the transition region, i.e. DF* ranging between 0.95 and 0.05, is considered: prior to vitrification DF* equals 1 and Eq. (17) diverges. The same approach for determining k_{D0} and C_1 was used for isothermal cure experiments at 120, 100, 70, and 60 °C. The parameter C_1 is nearly constant over the temperature range. Plotting the

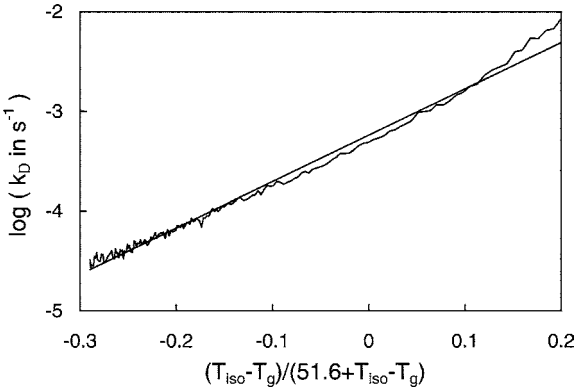

Fig. 3. The diffusion rate constant k_D vs. $(T_{\text{iso}}-T_g)/(51.6+T_{\text{iso}}-T_g)$ for the quasi-isothermal cure of the epoxy–anhydride system at $T_{\text{iso}}=85$ °C (see Eq. (14)). The straight line results from a linear regression.

$\log_{10} k_{D0}$ against the reciprocal cure temperature gives an Arrhenius-type temperature dependence for the temperature range studied (Fig. 4). This justifies the use of Eq. (14). The activation energy of k_{D0} is ca. 110 kJ mol^{-1}.

3.2.3. Reaction kinetics modeling

One approach could be to employ only isothermal cure data to estimate: (1) the parameters for the chemical rate equation (Eq. (5)) from heat flow data before vitrification and (2) the parameters for the diffusion rate constant k_D (Eq. (14)) using the method

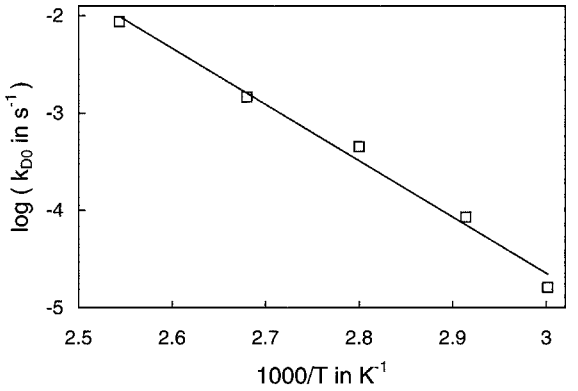

Fig. 4. Diffusion rate constant k_{D0} vs. the reciprocal of the isothermal cure temperature for the epoxy–anhydride system cured at various temperatures. The straight line results from a linear regression.

discussed in the previous paragraph. The parameters for the T_g–x relation can be determined from residual cure experiments. Although this approach is possible, the prediction is only accurate over the relatively narrow temperature range that was used to derive the parameters (60–120 °C). Taking non-isothermal experiments with pronounced mobility restrictions into account, the temperature range can be largely extended.

Therefore, a non-linear multiple parameter regression method was used to derive an optimum set of parameters by minimizing the sum of squares of the differences between measured and calculated values for an extended range of both isothermal and non-isothermal conditions. The experimental data used for optimizing the model parameters are:

$$\left(\frac{\mathrm{d}x}{\mathrm{d}t}(x,T)\right)_{\mathrm{obs}} = \frac{1}{\Delta H_{\mathrm{tot}}}\frac{\mathrm{d}H}{\mathrm{d}t}\Big|_{\mathrm{NR\ \ heat\ \ flow,obs}} \quad (18)$$

$$\mathrm{DF}(x,T) \cong \mathrm{DF}^*(x,T) = \frac{C_p(x,T) - C_{pg}(x,T)}{C_{pl}(x,T) - C_{pg}(x,T)} \quad (19)$$

3.3. Modeling results for the epoxy–anhydride system

The isothermal cure experiments (60–120 °C) were optimized together with multiple non-isothermal cure experiments showing a marked effect of mobility restrictions (heating rates of 0.04, 0.2, and 0.4 °C min^{-1}). Note that it was impossible to quantitatively assess the reaction rate of the experiment at 0.04 °C min^{-1}: the heat flow due to reaction is below 100 μW (for a 10 mg sample) over a reaction time that exceeds 2 days. Nevertheless, the heat capacity signal is very clear and allows an accurate calculation of the mobility factor.

After optimization, the agreement between experimental data and the modeling results is very satisfactory (see Figs. 5–8), especially considering the wide range of experimental conditions and the fact that *all* heat capacity and non-reversing heat flow profiles are fitted with *one* parameter set.

For the rate of conversion curves small deviations are noted in the chemically controlled region. Because the chemical rate equation (Eq. (5)) was optimized simultaneously for a large range of experimental conditions (isothermal cure at 60–120 °C and non-isothermal cure at 2.5–15 °C min^{-1}), slightly larger deviations result for the individual experiments. Optimizing the model for a single experiment results in a better (mathematical) fit but with a reduced physical meaning of the parameters.

The sudden decrease in diffusion factor near vitrification is well described for both quasi-isothermal and non-isothermal conditions (Figs. 5 and 6). In the latter case, a similar level (degree of vitrification) is reached in-between vitrification and devitrification.

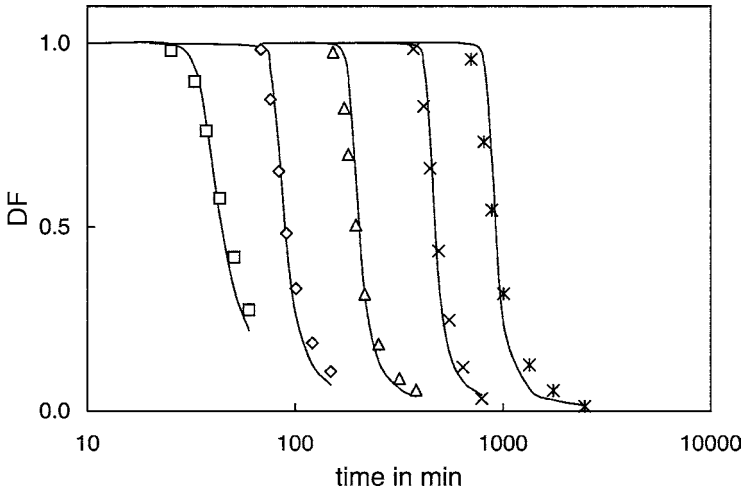

Fig. 5. Diffusion factor for the quasi-isothermal cure of an epoxy–anhydride system at: 120 °C (□); 100 °C (◇); 85 °C (△); 70 °C (×); 60 °C (✱). Data points from D(S)TMC (DF^*); optimized model (—).

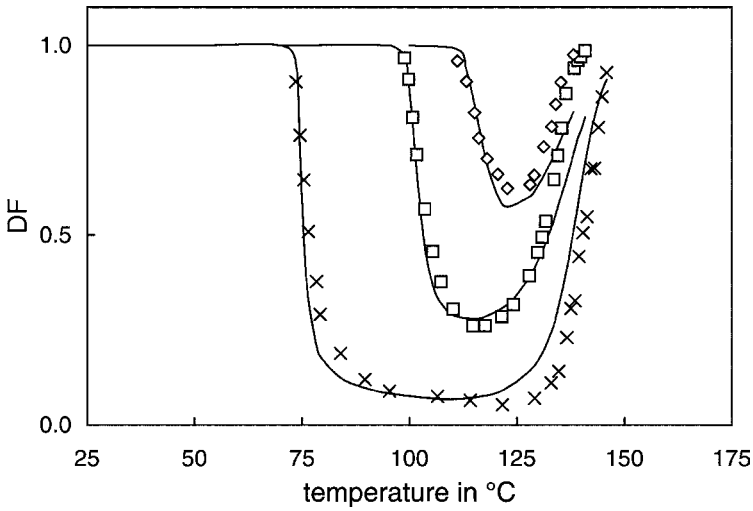

Fig. 6. Diffusion factor for the non-isothermal cure of an epoxy–anhydride system at: 0.04 °C min^{-1} (×); 0.2 °C min^{-1} (□); 0.4 °C min^{-1} (◇). Data points from D(S)TMC (DF*); optimized model (—).

Even the increase due to devitrification is properly predicted. Moreover, Figs. 7 and 8 illustrate well the effect of mobility limitations on the cure reaction under quasi-isothermal conditions (70 and 85 °C) and for a non-isothermal condition with a low heating rate (0.2 °C min^{-1}). The arrow in Fig. 7 indicates the point where the reaction rate is still totally chemically controlled. The thin dashed line simulates a chemically controlled experiment using the same model, but with DF fixed to unity. From the indicated point, a drop in the experimental reaction rate is observed, which is again very well described. Under non-isothermal conditions at 0.2 °C min^{-1} a shoulder of more or less constant reaction rate spanning a 40 °C temperature interval is noticed (Fig. 8). Simultaneously, the low value of the mobility factor is found (Fig. 6). This shows that under mobility-controlled conditions the proposed model permits the estimation of the level

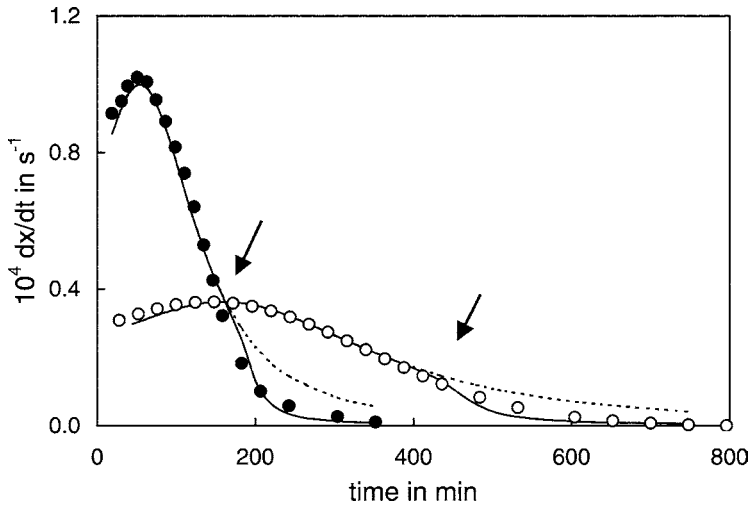

Fig. 7. Reaction rate for the quasi-isothermal cure of an epoxy–anhydride system. Data points from D(S)TMC at 70 °C (●) and 85 °C (○); optimized rate including diffusion control (—); simulated chemically controlled rate (- - -; Eq. (5)).

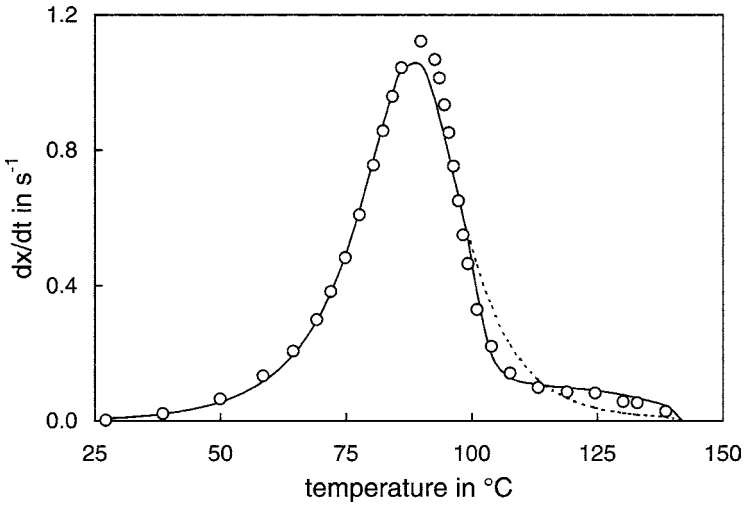

Fig. 8. Reaction rate for the non-isothermal cure of an epoxy–anhydride system at 0.2 °C min^{-1}: measured rate from D(S)TMC (○); optimized rate including diffusion control (—); simulated chemically controlled rate (- - -; Eq. (5)).

of both reaction rate and diffusion (mobility) factor and thus provides a description of the overall cure kinetics.

It is important to note that the model clearly demonstrates that the most critical factor determining whether a reaction is diffusion-controlled or not is the difference between the reaction temperature and the glass transition temperature. When T_g rises up to the curing temperature, chain segments become less mobile, which results in a mobility-restricted reduced reaction rate. Prior to vitrification (as long as $T - T_g$ exceeds 25 °C) the apparent rate constant, k_{app} equals the kinetic rate constant, k_{kin} ($k_D \gg k_{kin}$) and DF equals unity. On the contrary, diffusion becomes the limiting step when $k_{kin} \gg k_D$, which is the case when T_g nears the reaction temperature (in the vitrification zone). As a result, the reaction becomes diffusion-controlled and DF drops towards zero. A (near) zero value is reached when T_g becomes 15–20 °C higher than T. The latter condition occurs during isothermal curing over extended periods of time.

One should keep in mind that the mobility needed for diffusion of reactive groups toward each other is not restricted as a result of gelation. This is characteristic of diffusion which is not influenced by the existence of large scale molecular structures until these constitute effective topological constraints. For the epoxy–anhydride system, gelation occurs at 25% conversion (determined by dynamic rheometry), corresponding to a T_g of −20 °C.

Furthermore, it is worth noting that experiments occurring in chemically controlled conditions only (for high cure temperatures or low conversion) can be simulated correctly using the general cure rate law. This proves that effects of chemical and diffusion control are well separated, even outside the range of conditions for which the model was optimized.

3.4. Modeling results for the epoxy–amine system

For the epoxy–amine system an analogous approach has been applied. Again the three sets of parameters, one set for the chemical rate equation (Eq. (5)), one set for the diffusion rate constant (Eq. (14)), and for the T_g–x relation (Eq. (15)), were optimized using a combination of isothermal and non-isothermal experiments.

As seen in Fig. 9, the experimental and calculated DF profiles agree very well for the quasi-isothermal cure at reaction temperatures ranging from 25 to 100 °C. Compared to the epoxy–anhydride system, where the deceleration of the reaction rate caused by mobility restrictions was only noticed at the final stages of cure (Figs. 7 and 8), a tremendous decrease of the rate of reaction is already observed early in the epoxy–amine cure process (Figs. 10 and 11). For the

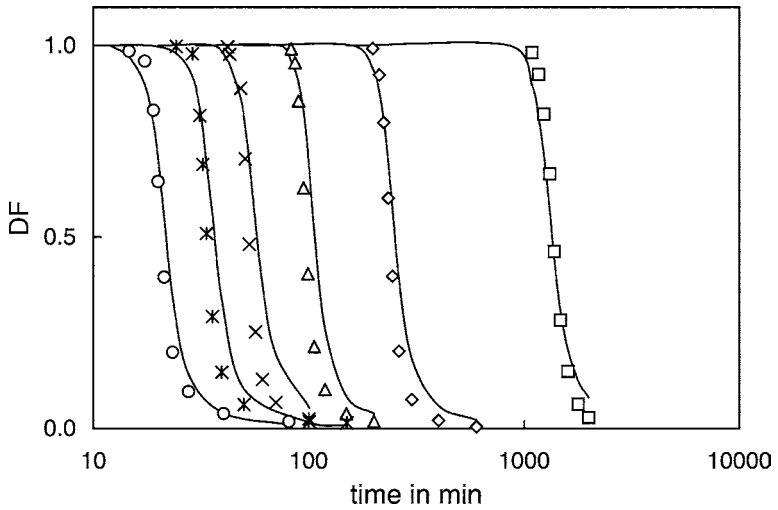

Fig. 9. Diffusion factor for the quasi-isothermal cure of an epoxy–amine system at: 100 °C (○); 90 °C (✱); 80 °C (×); 70 °C (△); 52 °C (◇); 25 °C (□). Data points from D(S)TMC (DF^*); optimized model (—).

isothermal cure at 90 and 100 °C (Fig. 10), the deviation from the chemically controlled rate (dashed line) already becomes pronounced near the maximum rate of reaction. The final conversion attained at these temperatures is about 75%: 25% of the reactive functionalities remain frozen out in the glass. Looking at the non-isothermal cure at 0.2 °C min^{-1} (Fig. 11), the chemical rate equation predicts a higher reaction rate even at the peak temperature. The temperature needs to be increased an additional 150 °C to reach full cure. The remarkable differences between the observed reaction rate and the calculated chemical reaction rate demonstrate the importance of the effect of mobility restrictions in these cases.

The epoxy–amine system is obviously more difficult to treat than the epoxy–anhydride system. The experimental conditions are more stringent (the temperature interval in which cure occurs exceeds 200 °C)

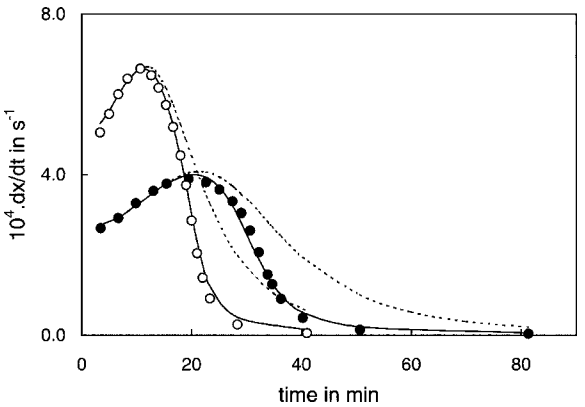

Fig. 10. Reaction rate for the quasi-isothermal cure of an epoxy–amine system. Data points from D(S)TMC at: 100 °C (○) and 90 °C (●); optimized rate (—); chemically controlled rate (- - -; Eq. (5)).

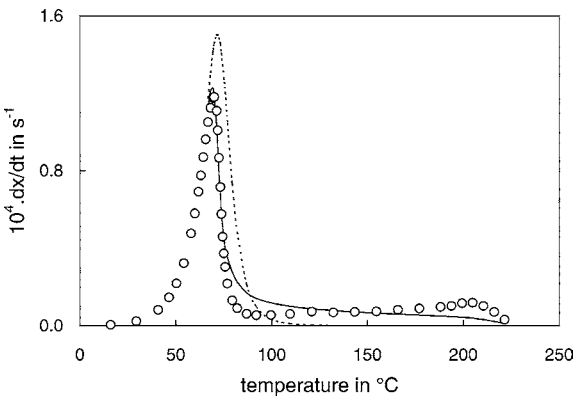

Fig. 11. Reaction rate for the non-isothermal cure of an epoxy–amine system at 0.2 °C min^{-1}: measured rate from D(S)TMC (○); optimized rate including diffusion control (—); simulated chemically controlled rate (- - -; Eq. (5)).

and the empirical kinetic rate equation is probably not accurate enough. However, the proposed approach allows the model to be refined without too much difficulty. An important advantage of the approach is the fact that the T_g–x relationship does not need to be known in advance. The experimental determination of the T_g–x relationship demands a lot of effort since it comprises T_g–x data derived from a series of residual cure experiments. Moreover, for the highly reactive epoxy–amine system, T_g for more advanced conversions cannot be easily measured in residual cure experiments. Indeed, as soon as the material (partially) devitrifies, the reaction restarts in diffusion-controlled conditions, and the material remains in the partially devitrified state (e.g. DF* ca. 0.2) up to full cure.

3.5. Evolution of the apparent activation energy from modeling

Toda et al. [40] presented an approach to estimate the evolution of an apparent (or overall) activation energy E_{app} from the contribution of the reaction exotherm to the imaginary component of the heat capacity. Schawe [39] extended this idea to calculate a diffusion factor DF from the heat flow phase signal (measured at a low frequency of 1/210 Hz), assuming a constant E_{app} in the chemically controlled part of the reaction.

E_{app} expresses the instantaneous temperature dependence of the reaction rate (evaluated at a fixed conversion, using an Arrhenius-type relation, see also Eqs. (5) and (7)). In this work, E_{app} was estimated from the model by calculating the change in the rate of conversion for a ± 1 K change in the reaction temperature. The results for the anhydride-cured and amine-cured epoxies are given in Fig. 12A and B, respectively. For the epoxy–anhydride, E_{app} is nearly constant up to the onset of vitrification. Subsequently, as DF decreases, a steep increase in E_{app} is noted. The autocatalytic behavior observed in Fig. 1 is due to an increase in the corresponding apparent pre-exponential factor A_{app}. For the epoxy–amine system, E_{app} first decreases with increasing reaction conversion, causing the (strong) autoacceleration (see Fig. 10). Subsequently, when the cure becomes diffusion-controlled (when DF decreases), E_{app} sharply increases, indicating the strong temperature dependency of DF (see Eqs. (7) and (8)). A similar increase was deduced by Schawe [39], interpreting non-isothermal DSC data using a model-free kinetics approach [23]. The results of the present paper emphasize again that E_{app} is usually not constant, even in the chemically controlled part of the cure reaction (see also Section 1). Some insight in the reaction mechanism can be gained from the evolution of the combination of A_{app} and E_{app} with conversion (and temperature), but only thorough modeling of the kinetics results in a reliable model.

3.6. Remarks concerning the proposed model and approach: influence of modulation frequency

The decrease in heat capacity due to vitrification occurs when the characteristic time-scale of molecular relaxations associated with the co-operative chain segment mobility becomes longer than the modulation

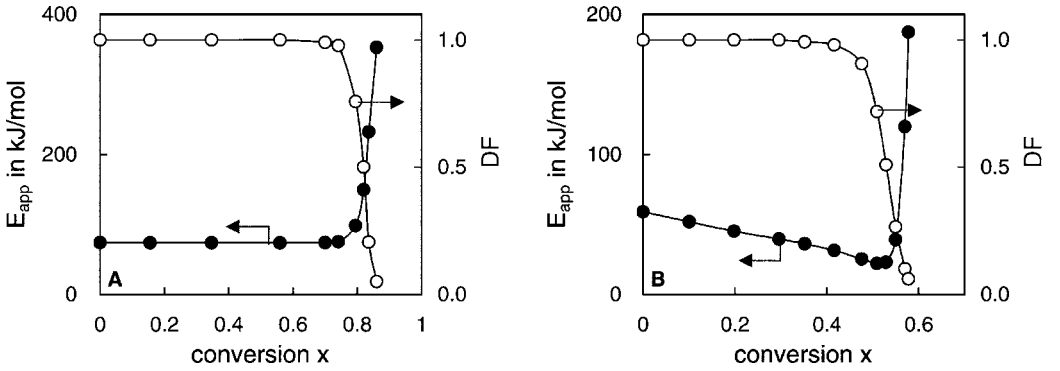

Fig. 12. Evolution of the apparent activation energy (●, from modeling) and the experimental diffusion factor (○, from D(S)TMC (DF*)) for the isothermal cure of: (A) an epoxy–anhydride system at 85 °C and (B) an epoxy–amine system at 70 °C.

period (or the characteristic time-scale of the experiment) [10]. If a higher modulation frequency is selected, the increasing relaxation time due to chemical reaction will interfere sooner with the modulation frequency and vitrification will be observed at a lower degree of conversion [41]. Note that the reaction rate itself depends on the average temperature and remains largely unaffected by the modulation frequency (in the currently available frequency range of 0.01–0.05 Hz).

The fact that DF*, for a (characteristic) modulation frequency f^* of 1/60 Hz, can be used as a model for DF for both amine and anhydride-cured epoxy systems indicates that the characteristic time for the co-operative chain segment mobility involved in the glass transition (region) measured at a frequency of 1/60 Hz, is comparable to the characteristic time of the (reaction) rate-determining mobility upon transition to diffusion-controlled reaction conditions. In other words, at vitrification, the mobility required for diffusion of reactive groups toward each other corresponds to the chain segment mobility displayed in the (normalized) heat capacity for the 'characteristic frequency' of 1/60 Hz.

For other thermosetting systems, even other epoxy-hardener systems, the rate-determining mobility upon transition to diffusion-controlled reaction conditions might correspond to the co-operative mobility frozen in at a (slightly) different characteristic frequency. Therefore, a study of the effect of frequency on the vitrification of resin systems related to their chemical structure and reaction mechanism might offer new insights concerning the interrelations between chemical reaction kinetics, vitrification, and diffusion control effects for different epoxy-hardener combinations.

Since the 'characteristic frequency' is not a priori known, a generalization of the modeling approach is needed. Consider the epoxy–anhydride system for which the (frequency-dependent) mobility factor MF(f) corresponds to the (frequency-independent) diffusion factor DF for $f = f^* = 1/60$ Hz. For an experiment performed at a frequency f different from f^*, the experimental mobility factor MF(f) would be shifted with respect to the diffusion factor DF = MF(f^*) = DF*.

The experimental mobility factor MF(f) can still be modeled using the same equations (Eqs. (11) and (14)), but for the T_g–x equation the shift in T_g with modulation frequency f needs to be taken into account. In the simplest case, the shift could be considered independent of the reaction conversion:

$$T_g(x,f) = \frac{T_{go} + ax}{1 - K_C X_C} + b \log\left(\frac{f}{f^*}\right) \tag{20}$$

where b is the shift in T_g for one decade in frequency (about 3–4 °C).

To model DF, Eq. (20) is evaluated with $f = f^*$, while for the evolution of the mobility factors MF their respective modulation frequency f is used. In this way, the information from experiments performed at different frequencies can be combined, and the characteristic frequency f^* becomes an additional optimized parameter. Note that in previous papers [5–7] the mobility factor at the characteristic frequency MF(f^*) is shortly termed mobility factor DF*.

4. Conclusions

Using the approach proposed, the cure kinetics can be modeled over the entire range of cure using D(S)TMC results only, as this technique quantitatively assesses conversion and reaction rate from the non-reversing heat flow signal as well as the mobility factor from the heat capacity signal. The latter allows predicting the decrease of reaction rate in the vitrification zone. The optimization procedure provides a unique set of kinetic, diffusion, and T_g–x model parameters that describes all experimental profiles in a broad range of isothermal and non-isothermal conditions.

A small modification or further extension of the model to account for the frequency dependency of the mobility factor would allow for a more detailed study of the interrelations between chemical structure, chemical kinetics, vitrification, and diffusion control.

More elaborated models concerning the reaction kinetics, diffusion limitations and the T_g–x relationship can be introduced without much effort and models proposed in literature can be readily evaluated [11,42–45]. For the cure study of radical reactions, such as the unsaturated polyester resin–styrene copolymerization, a different and more elaborated approach incorporating a molecular weight-dependent diffusion coefficient, should be employed to take the Trommsdorff or gel effect into account [9].

Acknowledgements

This work is part of the Ph.D. dissertation of Dr. A. Van Hemelrijck. G. Van Assche is a post-doctoral researcher of the Foundation for Scientific Research FWO, Flanders (Belgium). This research was also supported by the Institute for Scientific Technological Research IWT, Flanders (Belgium).

References

[1] R.B. Primes, in: E.A. Turi (Ed.), Thermal Characterisation of Polymeric Materials, Academic Press, New York, 1981, p. 435 (Chapter 5).
[2] J.M. Barton, Adv. Polym. Sci. 72 (1985) 111.
[3] R.A. Fava, Polymer 9 (1968) 137.
[4] G. Wisanrakkit, J.K. Gillham, J. Coat. Technol. 62 (1990) 35.
[5] G. Van Assche, A. Van Hemelrijck, H. Rahier, B. Van Mele, Thermochim. Acta 268 (1995) 121–142.
[6] G. Van Assche, A. Van Hemelrijck, H. Rahier, B. Van Mele, Thermochim. Acta 286 (1996) 209–224.
[7] G. Van Assche, A. Van Hemelrijck, H. Rahier, B. Van Mele, Thermochim. Acta 305 (1997) 317–334.
[8] S. Swier, G. Van Assche, A. Van Hemelrijck, H. Rahier, E. Verdonck, B. Van Mele, J. Thermal Anal. Cal. 54 (2) (1998) 585–604.
[9] G. Van Assche, E. Verdonck, B. Van Mele, Polymer 42 (7) (2001) 2959–2968.
[10] R. Scherrenberg, V. Mathot, P. Steeman, J. Thermal Anal. Cal. 54 (2) (1998) 477–499.
[11] K. Dusek, I. Havlisek, Prog. Org. Coat. 22 (1993) 145.
[12] M.R. Kamal, Polym. Eng. Sci. 14 (1974) 231.
[13] I. Mita, K. Horie, J. Macromol. Sci.-Rev., Macromol. Chem. Phys. C27 (1987) 91.
[14] K. Horie, I. Mita, Adv. Polym. Sci. 88 (1989) 77.
[15] E. Rabinowitch, Trans. Faraday Soc. 33 (1937) 1225.
[16] Y. Deng, G.C. Martin, Macromolecules 27 (1994) 5141.
[17] M. Gordon, W. Simpson, Polymer 2 (1961) 383.
[18] J.D. Ferry, Viscoelastic Properties of Polymers, 3rd Edition, Wiley, New York, 1961 (Chapter 11).
[19] I.M. Ward, Mechanical Properties of Solid Polymers, 2nd Edition, Section 7.4, Wiley, New York, 1983 (Chapter 7).
[20] J.M.G. Cowie, Polymers: Chemistry & Physics of Modern Materials, 2nd Edition, Section 12.11, Blackie, New York, 1991 (Chapter 12).
[21] M.L. Williams, R.F. Landel, J.D. Ferry, J. Am. Chem. Soc. 77 (1955) 3701.
[22] S. Vyazovkin, N. Sbirrazzuoli, Macromolecules 29 (1996) 1867.
[23] S. Vyazovkin, N. Sbirrazzuoli, Macromol. Chem. Phys. 200 (1999) 2294. (and references therein).
[24] E.A. DiMarzio, J. Res. Natl. Bur. Std., Sect. A 68A (1964) 611.
[25] A. Hale, C.W. Macosko, H.E. Bair, Macromolecules 24 (1991) 2610.
[26] G. Huybrechts, G. Van Assche, Comput. Chem. 22 (1998) 413.
[27] Subroutine VAO5A, Harwell Subroutine Library, Harwell.
[28] G. Huybrechts, Y. Hubin, B. Van Mele, Int. J. Chem. Kinet. 21 (1989) 575.
[29] J. Borchardt, F. Daniels, J. Am. Chem. Soc. 79 (1957) 41.
[30] R.B. Prime, Polym. Eng. Sci. 13 (1973) 365.
[31] T.W. Char, G.D. Shyu, A.I. Isayev, Rubber Chem. Technol. 66 (1994) 849.
[32] M. Reading, A. Luget, R. Wilson, Thermochim. Acta 238 (1994) 295.
[33] B. Wunderlich, Y. Jin, A. Boller, Thermochim. Acta 238 (1994) 277.
[34] M. Reading, Trends Polym. Sci. 1 (1993) 248.
[35] P.S. Gill, S.R. Sauerbrunn, M. Reading, J. Thermal Anal. 40 (1993) 931.
[36] M. Reading, D. Elliot, V.L. Hill, J. Thermal Anal. 40 (1993) 949.
[37] P.J. Haines, F.W. Wilburn, Thermal Methods of Analysis, Principles, Applications and Problems, 1st Edition, Section 3.10.3, Blackie, Glasgow, 1995 (Chapter 3).
[38] S. Montserrat, I. Cima, Thermochim. Acta 330 (1999) 189–200.
[39] J.E.K. Schawe, J. Thermal Anal. Cal. 64 (2001) 599.
[40] A. Toda, T. Arita, M. Hikosaka, J. Thermal Anal. Cal. 60 (2000) 821.
[41] G. Van Assche, B. Van Mele, Y. Saruyama, Thermochim. Acta 377 (2001) 125.
[42] G. Wisanrakkit, J.K. Gillham, J. Appl. Polym. Sci. 41 (1990) 2885.
[43] D.H. Kim, S.C. Kim, Polym. Bull. 18 (1987) 533.
[44] H. Stutz, J. Mertes, K. Neubecker, J. Polym. Sci., Polym. Chem. Ed. 31 (1993) 1879.
[45] H. Stutz, J. Mertes, J. Polym. Sci., Polym. Chem. Ed. 31 (1993) 2031.